Interhemispheric asymmetry in transient global warming: The role of Drake Passage

David K. Hutchinson,[1,2] Matthew H. England,[1,2] Agus Santoso,[1,2] and Andrew McC. Hogg[2,3]

Received 1 January 2013; revised 7 March 2013; accepted 7 March 2013; published 29 April 2013.

[1] Climate models predict that the Northern Hemisphere (NH) will warm faster than the Southern Hemisphere (SH) in response to increasing greenhouse gases, and observations show that this trend has already begun to occur. This interhemispheric asymmetry has largely been attributed to land-ocean differences between the hemispheres and Arctic sea ice melt, while the role of ocean currents in setting this asymmetry is less well understood. This study isolates the impact of an open Southern Ocean gateway upon the interhemispheric asymmetry in transient global warming by forcing a fully coupled climate model with an increasing CO_2 scenario with and without a land bridge across Drake Passage (DP). It is found that over the transient warming period, the NH-SH surface warming asymmetry is reduced in the DP closed case, by approximately 41% for sea surface temperature and approximately 6% for surface air temperature. In the DP open case, sea ice extent is far greater in the SH than in the DP closed case, whereas the sea ice response to warming in the NH is insensitive to whether or not DP is closed. These results illustrate that part of the interhemispheric asymmetry in surface warming is due to the Antarctic Circumpolar Current (ACC) thermally isolating Antarctica. The ACC limits ocean heat transport across the DP latitudes and allows a much greater coverage of sea ice in the Southern Ocean than would be the case in the absence of a circumpolar ocean.
Citation: Hutchinson, D. K., M. H. England, A. Santoso, and A. M. Hogg (2013), Interhemispheric asymmetry in transient global warming: The role of Drake Passage, *Geophys. Res. Lett.*, *40*, 1587–1593, doi:10.1002/grl.50341.

1. Introduction

[2] Global climate models show a strong interhemispheric asymmetry in the transient response of surface air temperature (SAT) to CO_2, with the Northern Hemisphere (NH) warming considerably faster than the Southern Hemisphere (SH) [*Meehl et al*., 2007]. This result has been well established through several decades of climate modeling [e.g., *Bryan et al*., 1988; *Manabe et al*., 1991; *Flato and Boer*, 2001] and has been found to be largely attributed to the greater coverage of ocean in the SH, yielding a higher effective heat capacity of the SH compared to the NH. Higher evaporative cooling over the oceans implies that warming is more rapid over land, further enhancing the interhemispheric asymmetry independently of ocean circulation differences. Yet ocean circulation differs markedly across the hemispheres, with the land mass geometry enabling a circumpolar flow around Antarctica, which could impact the warming response to rising greenhouse gases. This study focuses on the role of an open Southern Ocean gateway in regulating the hemisphere-scale response to global warming in a coupled climate model.

[3] Observations of warming in recent decades have confirmed that this warming asymmetry has already begun to occur. The HADCRUT4 data set [*Morice et al.*, 2012] has shown a steady trend from 1980 onward exhibiting much faster warming in the NH compared to the SH. Furthermore, the spatial pattern of SAT warming in the last 2 decades is broadly consistent with earlier global climate model predictions [*Manabe et al.*, 2011]. Observations of ocean warming have also indicated greater warming of sea surface temperature (SST) in the NH compared to the SH, though the magnitude of asymmetry is somewhat less than that in the SAT [*Levitus et al*., 2012]. *Levitus et al*.'s [2012] data also indicate that the ocean heat uptake and its asymmetry toward greater NH warming are largest in the Atlantic Ocean. The Pacific and Indian Oceans make smaller contributions to the net interhemispheric asymmetry. *Lee et al.* [2011] used simulations of 20th century warming to show that the North Atlantic Ocean heat content increase is more dependent on remote heating of the global ocean than local heating of the Atlantic. This result suggests that advection of heat into the North Atlantic by ocean currents is playing a major role in setting the asymmetry of SST warming.

[4] A further cause of warming asymmetry is the difference in polar climates. Antarctic sea ice trends have been nonuniform in recent decades, with a decline west of the Antarctic Peninsula and growth over the Ross Sea region [*Simpkins et al.*, 2012]. By contrast, seasonal melting of Arctic sea ice appears to be accelerating [*Wang and Overland*, 2009], allowing a strong ice-albedo positive feedback that exacerbates the warming and thus the asymmetry between hemispheres. Sea ice can also alter the polar warming response by insulating the air from warmer ocean temperatures below the ice.

[5] There are several additional factors which may influence the interhemispheric asymmetry of global warming. Sulfate aerosols are expected to cool the NH more than the SH [*Dufresne et al.*, 2005] and therefore reduce the warming

All supporting information may be found in the online version of this article.

[1]Climate Change Research Center, University of New South Wales, Sydney, New South Wales, Australia.
[2]ARC Centre of Excellence for Climate Systems Science, Sydney, New South Wales, Australia.
[3]Research School of Earth Sciences, Australian National University, Canberra, Australian Capital Territory, Australia.

Corresponding author: D. K. Hutchinson, Climate Change Research Center, Level 4 Mathews Building, University of New South Wales, Sydney 2052, NSW, Australia. (david.hutchinson@unsw.edu.au)

0094-8276/13/10.1002/grl.50341

asymmetry. Ozone may also play a role in the asymmetry, as the anthropogenic ozone hole has caused a trend toward the high-index polarity of the Southern Annular Mode [*Thompson et al.*, 2011], contributing to cooling over high southern latitudes. In the present study, no aerosols are included, and ozone concentrations are prescribed from observations and fixed in time [*Wang et al.*, 1995]; thus, we focus on ocean heat transport and heat capacity effects on the asymmetry, and the specific role of the Drake Passage (DP) gap.

[6] The Antarctic Circumpolar Current (ACC) provides a further possible mechanism for slowing global warming at high southern latitudes. The vigorous re-entrant flow of the ACC prevents any net upper ocean meridional geostrophic flow across DP, causing Antarctica to be 3–4°C cooler than it would otherwise be if DP were closed [*Toggweiler and Bjornsson*, 2000; *Sijp and England*, 2004]. Although the impacts of the ACC upon the climate have been investigated previously in ocean-only models [*Cox*, 1989; *Toggweiler and Samuels*, 1995], in intermediate complexity climate models [*Sijp and England*, 2004; *Sijp et al.*, 2009], and in idealized continental geometries [*Enderton and Marshall*, 2009], the DP effect has not been explored in a coupled climate model with realistic continental geometry. Here we investigate the hypothesis that the ocean, and particularly the ACC, plays a major role in controlling the interhemispheric asymmetry during transient global warming. We compare climate simulations with an open and closed DP under transient warming to demonstrate the influence of the ACC on this interhemispheric asymmetry.

2. Climate Model and Experimental Design

[7] This study implements the Commonwealth Scientific and Industrial Research Organisation Mark version 3L climate model (CSIRO Mk3L) Earth system model, comprising fully interactive ocean, atmosphere, land, and sea ice submodels [*Phipps*, 2010]. CSIRO Mk3L is designed for millennial climate simulations with ocean model resolution of 1.6° latitude × 2.8° longitude × 21 levels, and atmospheric model resolution of 3.2° latitude × 5.6° longitude × 18 pressure levels. The version used in this study includes an updated configuration of the Indonesian Archipelago as implemented by *Santoso et al.* [2012].

[8] Two sets of six-member ensemble simulations were run. The first set uses the standard coastline configuration, and the second set includes an extra land bridge to close the Drake Passage (DP), referred to respectively as the DP_{open} and DP_{clsd} simulations. The land bridge reduces the ocean surface area of the SH by only 0.2% and therefore makes negligible *direct* change to hemisphere-averaged surface properties such as albedo and heat capacity. Indirect changes can occur, for example, via differing sea ice distributions across the hemispheres. The DP_{open} simulations were initiated from a 2500 year pre-industrial control simulation with an atmospheric CO_2 concentration of 280 ppm. The DP_{clsd} control simulation was also initiated from this run at year 1500 and equilibrated for a further 2000 years with the DP land bridge included. A six-member ensemble was generated at the end of each control run, using the model restart configuration at the end of six consecutive years. Each ensemble member was then perturbed with increasing atmospheric CO_2 concentration following the Special Report on Emission Scenarios A2 forcing scenario [*Nakicenovic and Swart*, 2000] from nominal year 1781 until 2100. From the year 2100 onward, CO_2 was held fixed at 856 ppm.

[9] The control simulations and warming experiments were initially conducted with and without flux adjustments in single-member experiments. The flux adjustments were set in order to restore the DP_{open} simulation toward a modern climatology in the control state. The same set of flux adjustments were applied to the DP_{clsd} simulation for comparison. While the flux adjustments improved the climatology of the DP_{open} simulation, they produced spurious trends in the warming scenarios of the DP_{clsd} simulation. Since the DP_{clsd} simulation has a very different ocean circulation in the SH, the flux adjustments derived from the DP_{open} simulation restored the DP_{clsd} simulation toward a different mean state. Ensemble simulations were therefore run without flux adjustments to ensure a physically meaningful comparison between the two sets of simulations; their results are presented here.

3. Results

3.1. Interhemispheric Asymmetry

[10] The interhemispheric asymmetry in temperature anomaly (defined as the NH minus SH mean temperature anomaly) is plotted in Figure 1a, showing the SAT and SST asymmetry for both ensembles over the period 1781–2300. The SST asymmetry is higher in the DP_{open} ensemble than the DP_{clsd} ensemble, with an average asymmetry of 0.37°C from 2081-2100 in the DP_{open} ensemble, compared to 0.22°C in the DP_{clsd} ensemble. Using a bootstrap resampling method to obtain a 95% confidence interval, the SST asymmetry ensembles become statistically different from year 2072 onwards, marked by the vertical dashed line in Figure 1a. The asymmetry is mainly due to the reduced warming around the coast of Antarctica when DP is open (Figure 2c).

[11] [12] The spatial pattern and magnitude of asymmetry in SAT is more robust across the two ensembles (Figure 3); from 2081 to 2100, SAT asymmetry is 0.82°C in the DP_{open} ensemble compared to 0.77°C in the DP_{clsd} ensemble. The SAT asymmetry is thus more robust to the change induced by closing DP, suggesting that the differences in surface heat capacity and land-ocean effects are dominant in setting the SAT asymmetry. Nevertheless, the SAT asymmetry is reduced by 6% compared to the DP_{open} case, while the SST asymmetry is reduced by 41% compared to the DP_{open} case.

3.2. Surface Warming

[13] In the transient warming runs, SST anomalies around Antarctica remain considerably cooler in the DP_{open} ensemble over the Ross Sea and South Pacific sectors (Figure 2). The slower warming of SST around DP and in the Pacific sector of the Southern Ocean is likely due to the thermal isolation created by the ACC. There is also a region of enhanced warming in the Weddell Gyre to the east of DP, which warms faster in the DP_{open} ensemble. This region is associated with enhanced sea ice melt (Figure S1g in the auxiliary material). When DP is closed, this warmer region of the Weddell Gyre is spread across a larger area by the enhanced subpolar gyre that forms in the absence of the DP throughflow. The SST anomalies in the Arctic Ocean are very similar in both ensembles, showing relatively weak warming over most of the Arctic due to persistent sea ice

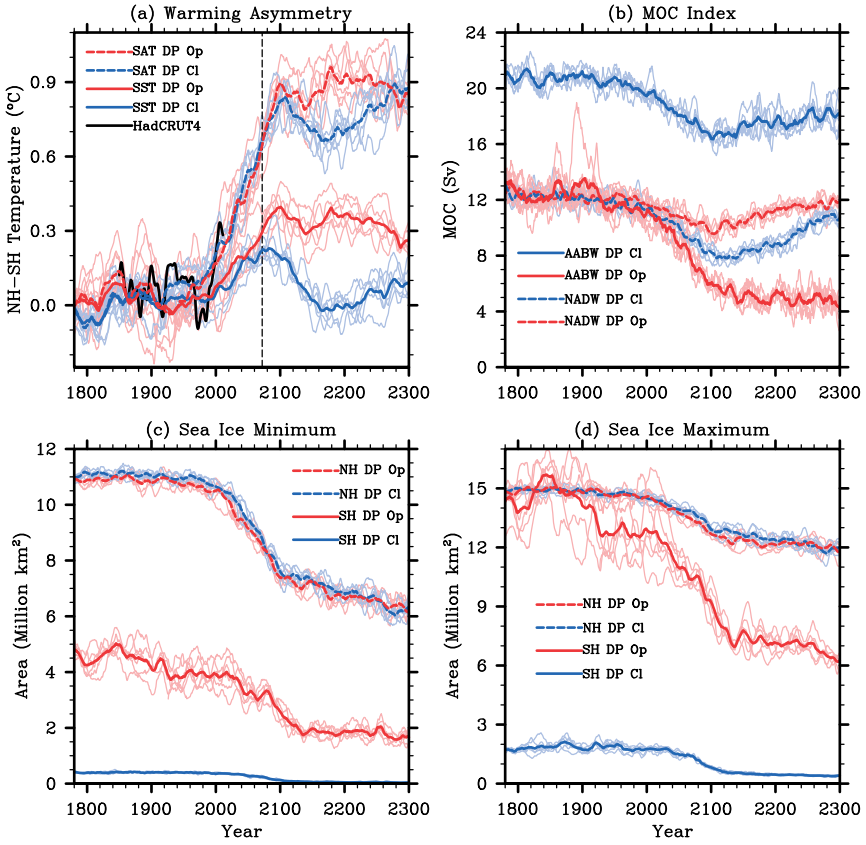

Figure 1. (a) Northern Hemisphere-Southern Hemisphere (NH-SH) temperature anomaly relative to the pre-industrial 100 year mean, showing the asymmetry in surface air temperature (SAT) anomalies (dashed lines), sea surface temperature (SST) anomalies (solid lines), and the HadCRUT4 observational data set [*Morice et al.*, 2012]. The vertical dashed line marks the year after which the SST asymmetry trends become statistically different. (b) Meridional overturning circulation (MOC) index calculated as the annual mean formation of Antarctic Bottom Water (AABW) (solid lines) and North Atlantic Deep Water (NADW) (dashed lines); (c) sea ice minimum extent, measured as the area where sea ice concentration is greater than 0.15 (NH—dashed lines, SH—solid lines); (d) as in Figure 1c but the sea ice maximum. In all plots, the bold lines represent ensemble means, and the fine lighter colored lines are the ensemble members. All model trends have been filtered using an 11 year running average.

coverage. There is also a localized region of very strong warming between Svalbard and Scandinavia, associated with sea ice melt. This "hotspot" is present in both ensembles and therefore appears to have little dependence on the DP changes in this experiment.

[14] The SAT changes show a similar pattern of polar amplification to that typical of International Panel on Climate Change (IPCC) AR4 simulations [*Meehl et al.*, 2007]. Figure 3 shows the SAT ensemble mean anomaly during 2081–2100 relative to the pre-industrial 100 year mean, as in Figure 2. Both ensembles show amplified warming in the high latitudes of the NH, especially in the Arctic, and stronger warming over land than ocean. SAT changes over the ocean reflect the SST patterns in most regions, except in the Arctic where there is little change in SST but a large increase in SAT. The SAT trends over the Arctic are broadly consistent with IPCC AR4 projections *Meehl et al.* [2007], while the SST warming in the Arctic is limited by persistent sea ice coverage, discussed further in section 3.4.

3.3. Deep Warming and Overturning Changes

[15] Figure 4 shows the zonally averaged ocean temperature anomaly for each ensemble, plotted as a function of latitude and depth during 2081–2100 relative to the pre-industrial 100 year mean. In the DP_{open} ensemble (Figure 4a), Southern Ocean warming is substantially weaker, especially adjacent to the coast of Antarctica. In the DP_{clsd} ensemble (Figure 4b), ocean warming persists through to the highest latitudes of the Southern Ocean, extending to approximately 1500 m depth. There is a reversal of this trend below 1500 m depth, with the DP_{open} ensemble warming more than the DP_{clsd} ensemble. This warming at depth can be explained by the shallower penetration of AABW in the DP_{clsd} ensemble, discussed below.

[16] [17] The meridional overturning circulation (MOC) streamfunction, calculated in density coordinates and reprojected back to latitude-depth space, during 2081–2100 is overlaid on the temperature anomalies in Figures 4a and 4b, with the difference in streamfunctions shown in Figure 4c. The rate of Antarctic Bottom Water (AABW) formation is higher in the DP_{clsd} ensemble; however, its density is reduced due to the warmer Antarctic climate. The lower density of the AABW mass causes it to penetrate to shallower depths, and the NADW mass becomes the dominant source of the abyssal ocean in this case. In the DP_{open} ensemble, by contrast, the AABW mass dominates the abyssal ocean.

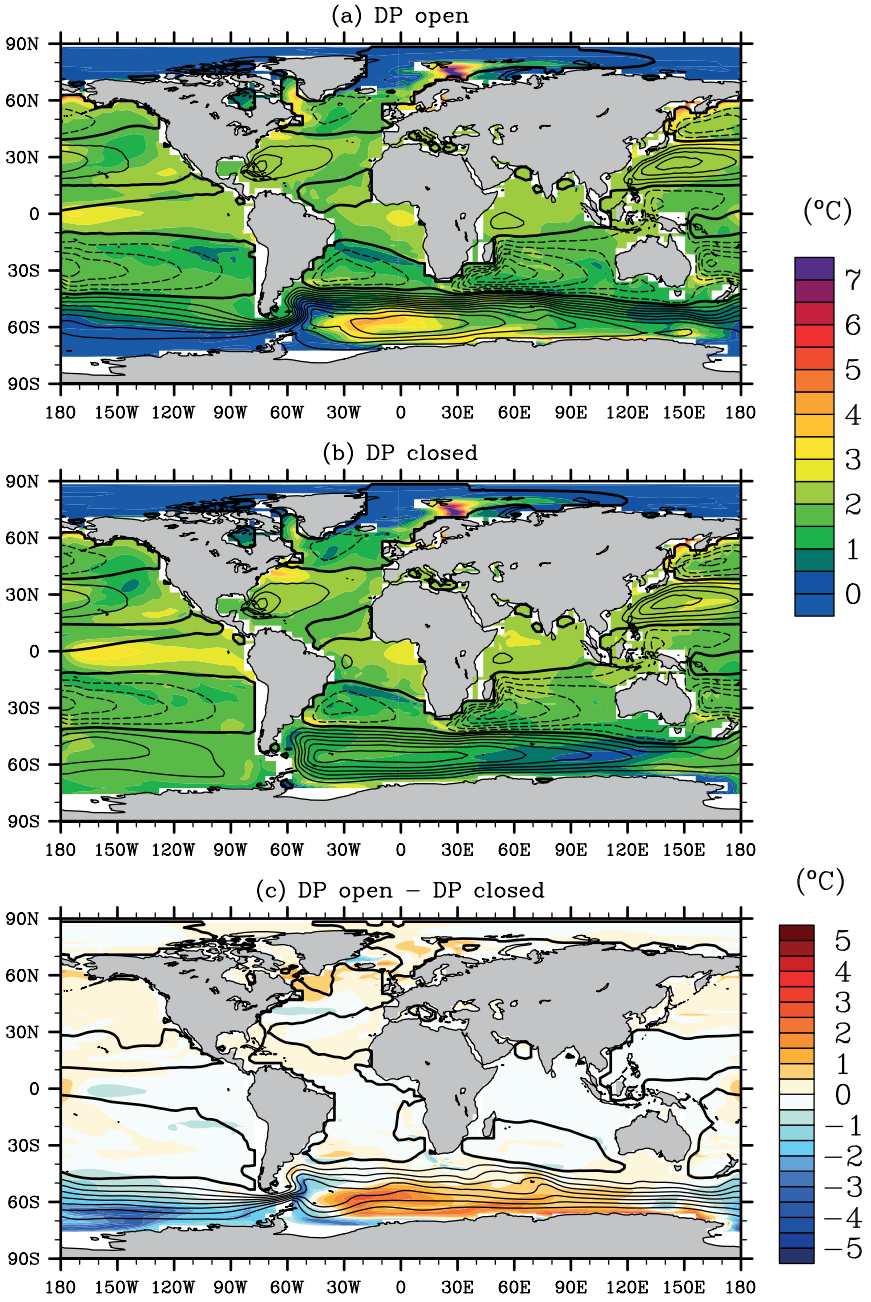

Figure 2. Sea surface temperature (SST) ensemble mean anomaly (colored contours) during 2081–2100 relative to the final 100 years of the pre-industrial simulation for (a) DP_{open}, (b) DP_{clsd}, and (c) the difference $DP_{open} - DP_{clsd}$. The respective barotropic streamfunctions during 2081–2100 are overlaid (black contours) on Figures 2a–2b, and the difference in streamfunctions is overlaid on Figure 2c. The streamfunction contour interval is 10 Sv, solid lines are positive, dashed lines are negative, and the zero contour is bold.

Therefore, AABW ventilation can more rapidly transfer any surface warming signal to the deep Southern Ocean in the DP_{open} ensemble, as seen in Figure 4c.

[18] [19] Figure 1b shows a time series of NADW and AABW formation, calculated from the MOC streamfunction in latitude-density coordinates. The domain of the water masses is defined as having potential density of $\sigma_2 >$ 35 kg m^{-3}, and poleward of 50°N and 50°S for NADW and AABW, respectively. Weakening of AABW relative to NADW formation in the DP_{open} ensemble slows the advection of heat across the DP latitudes. By contrast, the steady formation of AABW in the DP_{clsd} ensemble allows the high latitude Southern Ocean to warm more rapidly in that experiment set.

[20] [21] It is worth noting that the NADW formation is very similar between the two control simulations and does not appear to depend strongly on the DP throughflow, in contrast to previous studies that used models with idealized continental geometries [e.g., *Toggweiler and Bjornsson*, 2000; *Enderton and Marshall*, 2009] or a noninteractive atmosphere [*Sijp and England*, 2004]. The realistic landmass with topography and the fully interactive atmosphere

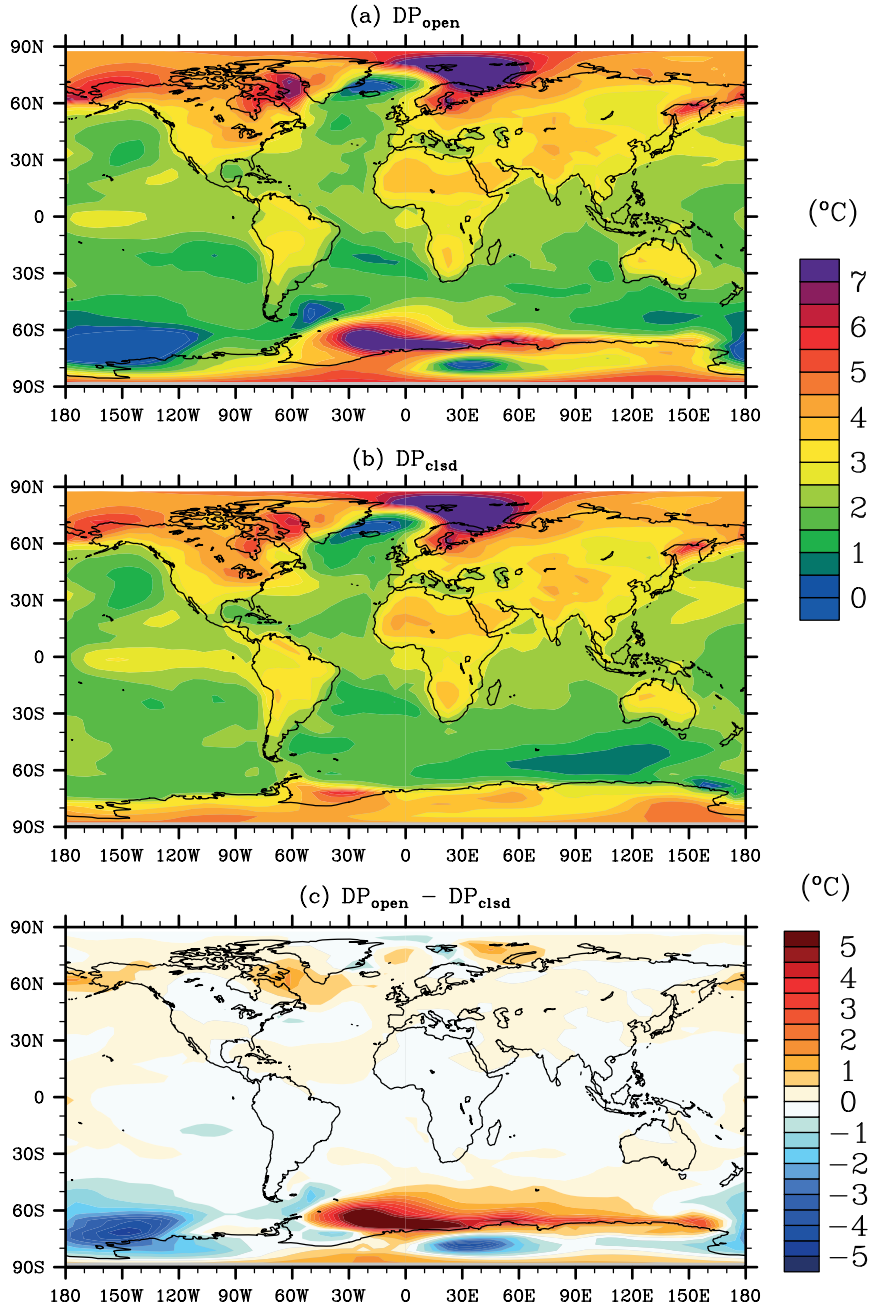

Figure 3. Surface air temperature anomaly during 2081–2100 relative to pre-industrial 100 year mean for (a) DP_{open}, (b) DP_{clsd}, and (c) the difference $DP_{open} - DP_{clsd}$.

in our model, complete with a hydrological cycle, appear to play an important role in regulating the heat and freshwater budgets of the Atlantic MOC [*Sinha et al.*, 2012]. Nonetheless, our result is consistent with *Rahmstorf and England* [1997], who showed that the rate of NADW formation is much less sensitive to Southern Ocean wind forcing when atmospheric thermal feedbacks are included.

3.4. Sea Ice Changes

[22] Differences in the Southern Ocean SST response of the two ensemble sets are strongly linked to sea ice patterns. The sea ice minima for both the NH and SH, measured respectively as the September and March sea ice extent (the area where sea ice concentration exceeds 0.15) are shown in Figure 1c. In the DP_{open} ensemble, the Arctic sea ice minimum is 11.0 M km^2 in pre-industrial conditions and declines to approximately 7.8 M km^2 by 2081–2100. The DP_{clsd} ensemble shows a similar trend, covering 11.1 M km^2 in pre-industrial conditions and declining to 8.0 M km^2 by 2081–2100. The Arctic sea ice maxima (Figure 1d) show a weaker decline over the same period, from 15.0 M to 13.0 M km^2 in the DP_{open} ensemble and 14.9 M to 13.3 M km^2 in the DP_{clsd} ensemble. Although the initial extent of the sea ice minimum is larger than satellite estimates (8.2 M km^2 for the 1980–1999 average), the magnitude of the decline in these simulations is consistent with IPCC AR4 projections [Figure 10.13 of *Meehl et al.*, 2007].

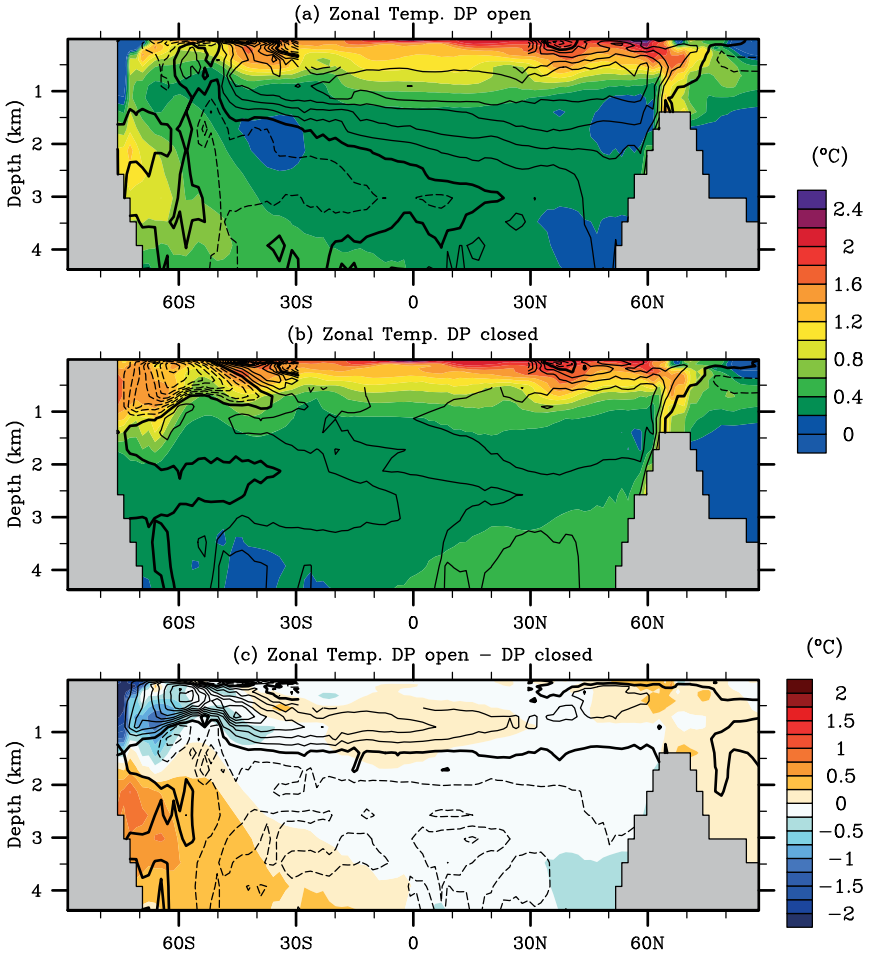

Figure 4. Zonal-averaged ocean temperature anomaly (colored contours) during 2081–2100 relative to pre-industrial 100 year mean, for (a) DP_{open}, (b) DP_{clsd}, and (c) $DP_{open} - DP_{clsd}$. The meridional overturning circulation during 2081–2100, calculated in density coordinates and reprojected back to latitude-depth space, is shown in black contours (2 Sv interval; solid lines are positive, dashed lines are negative, and the zero contour is bold). The tropical overturning cells are masked out in the domain ±30° latitude and < 500 m depth in order to show the near surface temperature trend.

[23] In the DP_{open} ensemble, there is a substantial coverage of SH sea ice, and though it decreases over the warming period, there remains a substantial coverage providing insulation to the sea surface despite ongoing global warming. The SH sea ice maximum declines from a pre-industrial level of 14.6 M to 9.7 M km^2 by 2081–2100, and the minimum declines from 4.4 M to 2.9 M km^2 over the same period, consistent with *Meehl et al.* [2007]. By contrast, the DP_{clsd} ensemble begins with almost no SH sea ice even in winter, with a pre-industrial maximum of 1.8 M km^2 declining to 1.0 M km^2 by 2081–2100, and a minimum declining from 0.4 M to 0.2 M km^2 over the same period.

[24] Recent observations show that Arctic sea ice is melting more rapidly than IPCC AR4 projections [*Wang and Overland*, 2009], and therefore, warming of SST in the Arctic is likely to be higher than our model suggests. Thus, our model may underestimate the asymmetry of warming in SST due to a weak trend in the Arctic. Nevertheless, the trends in Arctic sea ice are very similar between the DP_{open} and DP_{clsd} ensembles, and therefore, our experiments can still isolate the impact of the ACC on the warming asymmetry. For further details of the sea ice trends discussed here, polar stereographic plots of pre-industrial and late 21st century sea ice concentration for both ensemble sets can be found in Figure S1 for the SH and Figure S2 for the NH.

[25] The sea ice differences indicate that when the ACC is replaced by polar gyres in the presence of a land bridge, the increased advection of heat into the far Southern Ocean prevents much of the present day sea ice from forming. The sea ice coverage that forms when the ACC is present shields the subpolar Southern Ocean from substantial radiative forcing, thus slowing the warming response of the SH sufficiently to increase the interhemispheric asymmetry of both SST and SAT.

4. Summary and Conclusions

[26] The results presented here have further implications for detecting a CO_2 warming footprint in observed temperature trends. By comparing two sets of ensemble global warming simulations with an open and a closed DP, we demonstrate the importance of the ACC in limiting the rate of warming in the Southern Ocean. This effect would not be captured in climate models with simplified representations of the ocean, such as a uniform slab ocean or an aquaplanet. Furthermore, given the faster rate of warming in the NH and

the lower proportion of observations available in the high southern latitudes, care needs to be taken when inferring global trends from an asymmetric set of observations.

[27] This study has demonstrated the importance of the ACC in determining the climate response to global warming and highlights the need to improve its representation in climate models. While the impact of the DP has been analyzed in ocean-only, intermediate complexity and idealized coupled climate models, this study is the first to demonstrate its impact in a fully coupled climate model with realistic continents and a complete representation of the hydrological cycle. The present model relies upon subgrid scale eddy parameterizations; however, the Southern Ocean climate may respond differently when eddies are explicitly resolved [*Hallberg and Gnanadesikan*, 2006]. Investigating the interhemispheric asymmetry of global warming in eddy-permitting and eddy-resolving models will be the focus of a follow-up study.

[28] Transient global warming experiments with the DP closed reveal that a significant fraction of warming asymmetry in SST can be attributed to the thermal isolation provided the ACC. The ACC enables a much greater presence of sea ice and reduced poleward heat transport in the SH, causing the Southern Ocean as a whole to warm more slowly in response to strong CO_2 forcing. Previous discussions of the interhemispheric asymmetry have emphasized the role of heat capacity differences between the hemispheres, heat uptake in the deep mixed layers of the Southern Ocean, and ice-albedo feedback in the Arctic. This study has shown that the ACC provides a further mechanism to slow global warming in the high southern latitudes, contributing to a substantial proportion of the asymmetry compared to the scenario of a blocked circumpolar flow around the Southern Hemisphere.

[29] **Acknowledgments.** This work was supported by the Australian Research Council, including the ARC Centre of Excellence in Climate System Science, and an award under the Merit Allocation Scheme on the NCI National Facility at the ANU.

References

Bryan, K., S. Manabe, and M. J. Spelman (1988), Interhemispheric asymmetry in the transient response of a coupled ocean-atmosphere model to a CO_2 forcing, *J. Phys. Oceanogr.*, *18*(6), 851–867, doi:10.1175/1520-0485(1988)018<0851:IAITTR>2.0.CO;2.

Cox, M. D. (1989), An idealized model of the world ocean. Part I: The global-scale water masses, *J. Phys. Oceanogr.*, *19* (11), 1730–1752, doi:10.1175/1520-0485(1989)019<1730:AIMOTW>2.0.CO;2.

Dufresne, J.-L., J. Quaas, O. Boucher, S. Denvil, and L. Fairhead (2005), Contrasts in the effects on climate of anthropogenic sulfate aerosols between the 20th and the 21st century, *Geophys. Res. Lett.*, *32* (21), L21703, doi:10.1029/2005GL023619.

Enderton, D., and J. Marshall (2009), Explorations of atmosphere–ocean–ice climates on an aquaplanet and their meridional energy transports, *J. Atmos. Sci.*, *66*(6), 1593–1611, doi:10.1175/2008JAS2680.1.

Flato, G. M., and G. J. Boer (2001), Warming asymmetry in climate change simulations, *Geophys. Res. Lett.*, *28* (1), 195, doi: 10.1029/2000GL012121.

Hallberg, R., and A. Gnanadesikan (2006), The role of eddies in determining the structure and response of the wind-driven Southern Hemisphere overturning: Results from the modeling eddies in the Southern Ocean (MESO) project, *J. Phys. Oceanogr.*, *36*(12), 2232–2252, doi:10.1175/JPO2980.1.

Lee, S.-K., W. Park, E. van Sebille, M. O. Baringer, C. Wang, D. B. Enfield, S. G. Yeager, and B. P. Kirtman (2011), What caused the significant increase in Atlantic Ocean heat content since the mid-20th century?, *Geophys. Res. Lett.*, *38*(17), 1–6, doi:10.1029/2011GL048856.

Levitus, S., et al. (2012), World ocean heat content and thermosteric sea level change (0–2000 m), 1955–2010, *Geophys. Res. Lett.*, *39*(10), 1–5, doi:10.1029/2012GL051106.

Manabe, S., R. J. Stouffer, M. J. Spelman, and K. Bryan (1991), Transient responses of a coupled ocean-atmosphere model to gradual changes of atmospheric CO_2. Part I. Annual mean response, *J. Clim.*, *4*(8), 785–818, doi:10.1175/1520-0442(1991)004<0785:TROACO>2.0.CO;2.

Manabe, S., J. Ploshay, and N.-C. Lau (2011), Seasonal variation of surface temperature change during the last several decades, *J. Clim.*, *24*(15), 3817–3821, doi:10.1175/JCLI-D-11-00129.1.

Meehl, G., et al. (2007), *Global Climate Projections. In: Climate Change 2007: The Physical Science Basis. Contribution of Working Group I to the Fourth Assessment Report of the Intergovernmental Panel on Climate Change,* pp. 747–845, Cambridge University Press, Cambridge, U.K.

Morice, C. P., J. J. Kennedy, N. A. Rayner, and P. D. Jones (2012), Quantifying uncertainties in global and regional temperature change using an ensemble of observational estimates: The HadCRUT4 data set, *J. Geophys. Res.*, *117*(D8), 1–22, doi:10.1029/2011JD017187.

Nakicenovic, N., and R. Swart (eds.) (2000), *Special Report on Emissions Scenarios. A Special Report of Working Group III of the Intergovernmental Panel on Climate Change IPCC,* 570 pp., Cambridge University Press, Cambridge, U.K.

Phipps, S. J., (2010), The CSIRO Mk3L climate system model v1.2, 121pp., *Technical Report*, Antarctic Climate and Ecosystems Cooperative Research Centre, Hobart, Tasmania, Australia.

Rahmstorf, S., and M. H. England (1997), Influence of Southern Hemisphere winds on North Atlantic deep water flow, *J. Phys. Oceanogr.*, *27*(9), 2040–2054, doi:10.1175/1520-0485(1997)027<2040:IOSHWO>2.0.CO;2.

Santoso, A., M. H. England, and W. Cai (2012), Impact of Indo-Pacific feedback interactions on ENSO dynamics diagnosed using ensemble climate simulations, *J. Clim.*, *25*(21), 7743–7763, doi:10.1175/JCLI-D-11-00287.1.

Sijp, W. P., and M. H. England (2004), Effect of the Drake Passage throughflow on global climate, *J. Phys. Oceanogr.*, *34*(5), 1254–1266, doi:10.1175/1520-0485(2004)034<1254:EOTDPT>2.0.CO;2.

Sijp, W. P., M. H. England, and J. R. Toggweiler (2009), Effect of ocean gateway changes under greenhouse warmth, *J. Clim.*, *22*(24), 6639–6652, doi:10.1175/2009JCLI3003.1.

Simpkins, G. R., L. M. Ciasto, D. W. J. Thompson, and M. H. England (2012), Seasonal relationships between large-scale climate variability and Antarctic sea ice concentration, *J. Clim.*, *25*(16), 5451–5469, doi:10.1175/JCLI-D-11-00367.1.

Sinha, B., A. T. Blaker, J. J.-M. Hirschi, S. Bonham, M. Brand, S. Josey, R. S. Smith, and J. Marotzke (2012), Mountain ranges favour vigorous Atlantic meridional overturning, *Geophys. Res. Lett.*, *39*(2), 1–7, doi:10.1029/2011GL050485.

Thompson, D. W. J., S. Solomon, P. J. Kushner, M. H. England, K. M. Grise, and D. J. Karoly (2011), Signatures of the Antarctic ozone hole in Southern Hemisphere surface climate change, *Nature Geosci.*, *4*(11), 741–749, doi:10.1038/ngeo1296.

Toggweiler, J. R., and H. Bjornsson (2000), Drake Passage and palaeoclimate, *J. Quat. Sci.*, *15* (4), 319–328, doi:10.1002/1099-1417(200005)15:4<319::AID-JQS545>3.0.CO ;2-C.

Toggweiler, J. R., and B. Samuels (1995), Effect of Drake Passage on the global thermohaline circulation, *Deep Sea Res. I*, *42*(4), 477–500, doi:10.1016/0967-0637(95)00012-U.

Wang, M., and J. E. Overland (2009), A sea ice free summer Arctic within 30 years?, *Geophys. Res. Lett.*, *36*(7), 2–6, doi:10.1029/2009GL037820.

Wang, W.-C., X.-Z. Liang, M. Dudek, D. Pollard, and S. Thompson (1995), Atmospheric ozone as a climate gas, *Atmos. Res.*, *37*(1-3), 247–256, doi:10.1016/0169-8095(94)00080-W.